5252 *Chem. Mater.* **2009,** *21,* 5252–5257
DOI:10.1021/cm902247k

CHEMISTRY OF MATERIALS
Article

Synthesis of Highly Monodispersed Mesoporous Tin Oxide Spheres

Narihito Tatsuda,*,† Tadashi Nakamura† Daisuke Yamamoto,‡ Tatsufumi Yamazaki,‡ Tetsuya Shimada,‡ Haruo Inoue,‡ and Kazuhisa Yano*,†

†*Toyota Central Research & Development Laboratories, Incorporated, Nagakute, Aichi 480-1192, Japan, and* ‡*Department of Applied Chemistry, Graduate School of Urban Environmental Sciences, Tokyo Metropolitan University, 1-1 minami-Osawa, Hachioji, Tokyo, 192-0397 (Japan)*

Received July 22, 2009. Revised Manuscript Received October 2, 2009

Synthesis of monodispersed mesoporous tin oxide spheres and fabrication of close-packed mesoporous tin oxide opal is presented. By taking advantage of the oxidation of tin(II) chloride on the surface of monodispersed starburst carbon spheres (MSCS), which are produced using monodispersed mesoporous silica spheres as a host, nanocrystals of tin oxide accumulate into mesopores of MSCS. Calcination of the MSCS/SnO_2 composite yields monodispersed mesoporous tin oxide spheres (MMTOS) that consist of SnO_2 nanocrystals. Although the starburst structure of MSCS is lost during calcination, monodispersed spherical shape is retained. As a result of its uniformity, MMTOS can be self-assembled into a close-packed opal, which exhibits a stop band in the visible region.

Introduction

Monodispersed particles that have a uniform particle diameter can be self-assembled into a three-dimensional colloidal photonic crystal. The presence of photonic band gap due to the periodic modulation of the refractive index in a photonic crystal brings about the confinement of the propagation of light. Thus, optical applications, such as waveguides,[1] optical fibers,[2] nanocavities,[3,4] and low threshold lasers[5,6] could be expected. There have been many reports regarding the fabrication and application of colloidal photonic crystals; however, most of the efforts have been made using polystyrene latex or Stöber silica spheres.

We have developed monodispersed mesoporous silica spheres, termed as MMSS hereafter, that have highly monodisperse particle diameter and pore size.[7−9] High monodispersity and uniform mesopores of MMSS enable us to create a colloidal crystal with new function. The wavelength of the light reflected from the colloidal crystal fabricated from MMSS changed drastically depending on the relative pressure of water or benzene vapor.[10,11] When an emission dye was confined into mesopores of MMSS, laser oscillation could be attained due to the stop band effect.[12] Various types of nanoparticles or organic dyes can be incorporated into the mesopores of MMSS,[13−15] and it can be expected that the colloidal photonic crystal fabricated from the composite MMSS would function as novel photonic materials. However, since MMSS is not electrically conductive, the application of MMSS or its composite is obviously limited.

Recently, the templated synthesis of various types of mesoporous metal oxides by using mesoporous silicas or carbons as a host have been reported in large numbers.[16] Two techniques are mainly used for the preparation of them. One is a wet impregnation technique in which a metal salt solution is used, and the other is an incipient wetness technique in which metal alkoxide is used as a precursor. Mesoporous metal oxides, such as CeO_2,[17] Co_3O_4,[18] Fe_2O_3,[19] TiO_2,[20] and SnO_2,[21] have been synthesized with the methods. Among

*Corresponding authors. (N.T.) E-mail: e0848@mosk.tytlabs.co.jp. Tel: +81-561-71-7693. Fax: +81-561-63-6137. (K.Y.) E-mail: k-yano@mosk.tytlabs.co.jp. Tel: +81-561-71-7570. Fax: +81-561-63-6137.

(1) Tsuji, Y.; Morita, Y.; Hirayama, K. *IEEE Photonics Technol. Lett.* **2006**, *18*, 2410.
(2) Kuhlmey, B. T.; McPhedran, R. C. *Phys. B: Condens. Matter* **2007**, *394*, 155.
(3) Englund, D.; Fattal, D.; Waks, E.; Solomon, G.; Zhang, B.; Nakaoka, T.; Arakawa, Y.; Yamamoto, Y.; Vuckovic, J. *Phys. Rev. Lett.* **2005**, *95*, 013904.
(4) Yoshie, T.; Scherer, A.; Hendrickson, J.; Khitrova, G.; Gibbs, H. M.; Rupper, G.; Ell, C.; Shchekin, O. B.; Deppe, D. G. *Nature* **2004**, *432*, 200.
(5) Noda, S. *Science* **2006**, *314*, 260.
(6) Sakoda, K.; Ohtaka, K.; Ueta, T. *Opt. Express* **1999**, *4*, U1.
(7) Yano, K.; Fukushima, Y. *J. Mater. Chem.* **2003**, *13*, 2577.
(8) Yano, K.; Fukushima, Y. *J. Mater. Chem.* **2004**, *14*, 1579.
(9) Nakamura, T.; Mizutani, M.; Nozaki, H.; Suzuki, N.; Yano, K. *J. Phys. Chem. C* **2007**, *111*, 1093.
(10) Yamada, Y.; Nakamura, T.; Ishi, M.; Yano, K. *Langmuir* **2006**, *22*, 2444.
(11) Yamada, Y.; Nakamura, T.; Yano, K. *Langmuir* **2008**, *24*, 2779.
(12) Yamada, H.; Nakamura, T.; Yamada, Y.; Yano, K. Adv. Mater. DOI: 10.1002/adma.200900721
(13) Nakamura, T.; Yamada, Y.; Yano, K. *J. Mater. Chem.* **2006**, *16*, 2417.
(14) Mizutani, M.; Yamada, Y.; Nakamura, T.; Yano, K. *Chem. Mater.* **2008**, *20*, 4777.
(15) Nakamura, T.; Yamada, Y.; Yano, K. *J. Mater. Chem.* **2007**, *17*, 3726.
(16) Tiemann, M. *Chem. Mater.* **2008**, *20*, 961.
(17) Shen, W.; Dong, X.; Zhu, Y.; Chen, H.; Shi, J. *Microporous Mesoporous Mater.* **2006**, *85*, 157.
(18) Dickinson, C.; Zhou, W.; Hodgkins, R. P.; Shi, Y.; Zhao, D.; He, H. *Chem. Mater.* **2006**, *18*, 3088.
(19) Jiao, F.; Harrison, A.; Jumas, J. C.; Chadwick, A. V.; Kockelmann, W.; Bruce, P. G. *J. Am. Chem. Soc.* **2006**, *128*, 5468.
(20) Dong, A.; Ren, N.; Tang, Y.; Wang, Y.; Zhang, Y.; Hua, W.; Gao, Z. *J. Am. Chem. Soc.* **2003**, *125*, 4976.
(21) Smått, J. H.; Weidenthaler, C.; Rosenholm, J. B.; Lindén, M. *Chem. Mater.* **2006**, *18*, 1443.

 Published on Web 10/15/2009

them, mesoporous tin oxide has considerable potential for a variety of applications, such as a dye sensitized solar cell, an electrode for Li battery, and a sensor.

The preparation of mesoporous tin oxide by means of a soft-templating method using an alkylammonium salt as a surfactant has been reported. In the syntheses, tin(IV) chloride or tin tetraethoxide was used for a tin oxide precursor.[22,23] By using heat-resistant block-copolymer as a template, a highly crystalline mesoporous tin oxide film has been synthesized.[24] Mesoporous tin oxide spheres that consist of tin oxide nanoparticles were obtained by an alternative method.[25] A sol of tin oxide nanoparticles was mixed with furfral, and then organic components were removed. A hard-templating method was also employed to obtain mesoporous tin oxide.[26] A solution of tin(IV) chloride was introduced into mesopores of SBA-15, followed by heating and silica dissolution. However, to date, no report has been made of the synthesis of monodispersed mesoporous tin oxide spheres that are uniform enough to self-assemble into opal structure.

The purpose of the work described herein is to synthesize monodispersed mesoporous tin oxide spheres that are uniform enough to self-assemble into an opal structure and to evaluate their structural and electrical properties. By taking advantage of the oxidation of tin(II) chloride on the surface of monodispersed starburst carbon spheres,[27] which had been produced using MMSS as a host, monodispersed mesoporous tin oxide spheres have been synthesized. Incorporation of a porphyrin complex into mesopores of the tin oxide spheres led to the generation of photocurrent. Furthermore, high monodispersity of the spheres enables us to fabricate a three-dimensional colloidal photonic crystal from tin oxide spheres for the first time.

Experimental Section

Synthesis of MMTOS. Monodispersed mesoporous tin oxide spheres (MMTOS) were synthesized via a two-step nanocasting route as depicted in Scheme 1. Monodispersed mesoporous silica spheres (MMSS) obtained by the pore expansion method were used as a starting material.[14] Monodispersed starburst carbon spheres (MSCS) were first synthesized from MMSS[27] and used as a hard template for the synthesis of MMTOS. On the surface of MSCS, Sn^{2+} deposited as SnO_2 nanocrystal through the oxidation in an acidic media. Then the removal of MSCS by calcination yields MMTOS. A typical synthesis procedure is as follows. We modified Cao's procedure.[28] A 100 mg portion of MSCS was dispersed into the solution containing 250 mL of distilled water, 4 mL of conc. HCl, and 5.0 g of $SnCl_2$, which were purchased from Wako Co. Ltd. and used without further purification. This solution was stirred for 4 h at room temperature, followed by filtration and rinse with distilled water twice, and the MSCS/SnO_2 composite was obtained. Calcination of the MSCS/SnO_2 composite was carried out at 623 K for 12 h or 823 K for 6 h in air to obtain MMTOS.

Fabrication of a Colloidal Crystal. The fabrication of a colloidal photonic crystal is as follows: 0.1 g of MMTOS with the diameter of 322 nm was dispersed in 25 g of 1 g/L poly(diallyldimethylammonium chloride) (abbreviated as PDADMAC) aqueous solution containing 0.5 mol/L sodium chloride under stirring for 20 min. Excess PDADMAC was removed by twice repeating a cycle of centrifugation (5000 rpm, 10 min) and water washing. Afterward, the PDADMAC-coated spheres were dispersed in 25 g of 1 g/L poly(sodium 4-styrenesulfonate) (abbreviated as PSS) aqueous solution containing 0.5 mol/L sodium chloride, and PSS was deposited onto the PDADMAC-coated spheres in a similar way using the same conditions. Then the polyelectrolyte-coated MMTOS spheres were dispersed in water (1 wt %). After continuous stirring for 1 h, a sufficiently dispersed suspension was dropped onto a flat quartz plate, to form a close-packed array.

Photocurrent Measurement. Sn-TCPP/MMTOS film for a photocurrent generation measurement was obtained as follows. First, 5 g of ethanol, 0.2 g of acetyl acetone, 0.1 g of Triton X, and two drops of nitric acid were mixed. To 100 μL of the mixture was added 1 mg of MMTOS, and the suspension was sonicated for 10 min. Then a portion of the suspension was casted onto FTO glass (2 × 2 cm). After heating in air at 400 °C for 1 h, the glass coated with MMTOS was immersed in a saturated ethanol solution of tin tetra(carboxyphenyl)-porphyrin (Sn-TCPP) for 1 day at room temperature. A diffusion reflection spectrum was obtained with a Shimadu UV-3150 spectrophotometer. A fluorescence spectrum was measured using a Jasco EP-6500 spectrophotofluorometer. The Sn-TCPP/MMTOS film was soaked in 0.1 M NaOH solution to extract Sn-TCPP. The amount of Sn-TCPP was estimated to be 9.8×10^{-9} mol from the absorbance of the extract solution using an absorption constant of 5.83×10^5.

Photocurrent measurement of the Sn-TCPP/MMTOS film was conducted using a Hokuto Denko HA1010 mM1A electrochemical system. A sample was mounted on a specially designed cell equipped with an Ag/Ag^+ reference electrode and a platinum counter electrode. The measurement was conducted in acetonitrile containing 0.2 M tetra-*n*-propyl ammonium iodide and 0.1 M tetra-*n*-butyl ammonium hexafluorophosphate. Argon bubbling was carried out for 30 min before the measurement to remove oxygen from the solution. The light from a Ushio SX-UI500XQ Xe Lamp with an IR-cut filter was irradiated to the sample. The wavelength of the light was adjusted to 420 nm using an interference filter. The amount of light and illumination area were 1.70 mW/cm^2 and 3.14 cm^2, respectively.

Characterization. The MSCSs, MSCS/SnO_2 composites, and MMTOSs were observed under a transmission electron microscope (TEM), JEOL JEM-2000EX, and a scanning electron microscope (SEM), Akashi-Seisakusho SIGMA-V, to confirm their morphology. X-ray diffraction (XRD) patterns for the MSCS/SnO_2 composites and MMTOSs were obtained with a Rigaku RINT TTR with Cu Kα radiation to evaluate the structures of the crystalline SnO_2. The pore characteristics of MSCS/SnO_2 composite and MMTOSs were examined by means of nitrogen adsorption−desorption isotherms at 77 K, which were obtained with a Bell. Co. BELSORP-mini II. The samples were degassed at 423 K in 10^{-6} Torr for 2 h prior to each

(22) Wagner, T.; Kohl, C.-D.; Fröba, M.; Tiemann, M. *Sensors* **2006**, *6*, 318.
(23) Srivastava, D. N.; Chappel, S.; Palchik, O.; Zaban, A.; Gedanken, A. *Langmuir* **2002**, *18*, 4160.
(24) Brezesinski, T.; Fischer, A.; Iimura, K.; Sanchez, C.; Grosso, D.; Antonietti, M.; Smarsly, B. M. *Adv. Funct. Mater.* **2006**, *16*, 1433.
(25) Demir-Cakan, R.; Hu, Y.-S.; Antonietti, M.; Maier, J.; Titirici, M.-M. *Chem. Mater.* **2008**, *20*, 1227.
(26) Kim, H.; Cho, J. *J. Mater. Chem.* **2008**, *18*, 771.
(27) Nakamura, T.; Yamada, Y.; Yano, K. *Microporous Mesoporous Mater.* **2009**, *117*, 478.
(28) Cao, Y.; Cao, J.; Liu, J.; Zheng, M.; Shen, K. *Chem. Lett.* **2007**, *36*, 254.

adsorption measurement. The specific surface area of a sample was determined by the BET method. The pore size distribution was determined by the Barrent−Joyner−Hallender (BJH) method using the adsorption branch. The total pore volume was determined from the adsorbed amount of nitrogen at $P/P_0 = 0.95$.

Results and Discussion

Synthesis of Monodispersed Mesoporous Tin Oxide Spheres. Our strategy to synthesize monodispersed mesoporous tin oxide spheres (MMTOS) is depicted in Scheme 1. Monodispersed starburst carbon spheres (MSCS) are obtained by nanocasting using MMSS as a host.[27] Oxidation of Sn^{2+} at the surface of MSCS generates tin oxide, resulting in the formation of MSCS/SnO_2 composite spheres. Then, calcination of the MSCS/SnO_2 composite yields monodispersed mesoporous tin oxide spheres (MMTOS).

Figure 1 shows SEM images of MSCS and resultant MMTOSs obtained by calcination at 623 K and 823 K, respectively. Average particle sizes and coefficient of variations (CV) of these samples are summarized in Tables 1. The particles shrank approximately 20% during calcination. The average particle size decreased from 860 nm (MSCS) to 700 nm and 690 nm when calcined at 623 and 823 K, respectively. However, the monodispersity of MMTOS was still high even after calcination, and the CVs were 3.7% and 4.6% for the samples calcined at 623 K and 823 K, respectively.

TEM images of the MSCS/SnO_2 composite and MMTOSs are also shown in Figure 1. TEM observation reveals that nanoparticles less than 3 nm are homogeneously dispersed through the MSCS/SnO_2 composite, while nanoparticles with larger sizes are observed for MMTOSs. From the TEM images, crystalline sizes of MMTOSs calcined at 623 and 823 K are found to be 3−7 nm and 10−20 nm, respectively. MSCS consists of carbon nanorods with starburst structure.[27] During the calcination, carbon nanorods were removed by combustion, generating nanospace between SnO_2 nanocrystals. Then, the nanocrystals aggregated and became larger SnO_2 particles depending on the calcination temperature. It is surprising that monodispersed spherical morphology was still retained even though aggregation of SnO_2 nanocrystals occurred during the calcination.

Figure 2A shows the XRD patterns for the MSCS/SnO_2 composite and MMTOSs. Very broad weak peaks are observed at 2θ of 27, 34, and 53° in the XRD pattern for the MSCS/ SnO_2 composite, which are corresponding to the diffraction of 110, 101, and 211 planes of SnO_2 crystal, respectively. It was confirmed that SnO_2 nanocrystals formed in the MSCS/SnO_2 composite by considering the broadness of the peaks. The SnO_2 nanocrystals are assumed to deposit on the surface of

Scheme 1. Nanocasting Route To Obtain MMTOS[a]

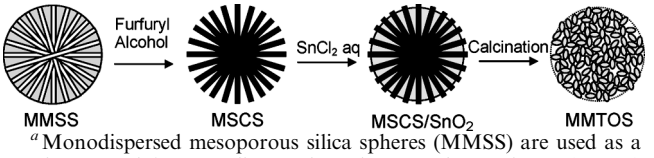

[a] Monodispersed mesoporous silica spheres (MMSS) are used as a starting material. Monodispersed starburst carbon spheres (MSCS) obtained from MMSS are immersed in an aqueous solution of $SnCl_2$. Oxidation of Sn^{2+} results in the formation of SnO_2 in the space of MSCS. A resultant MSCS/SnO_2 composite is calcined at the given temperature, yielding monodispersed mesoporous tin oxide spheres (MMTOS) that consist of SnO_2 nanocrystals.

Table 1. Properties of Samples

samples	particle size, nm	CV, %	pore volume, mL g^{-1}	specific surface area, m^2 g^{-1}	pore diameter, nm	crystalline size,[a] nm
MSCS	860	3.3	0.84	1560	1.8	
MSCS/SnO_2 composite	860	7.4	0.087	129	< 1.0	2.1
MMTOS calcined at 623 K	700	3.7	0.19	103	6.3	4.7
MMTOS calcined at 823 K	690	4.6	0.17	35	18	10.2

[a] Estimated by means of the Scherrer equation.

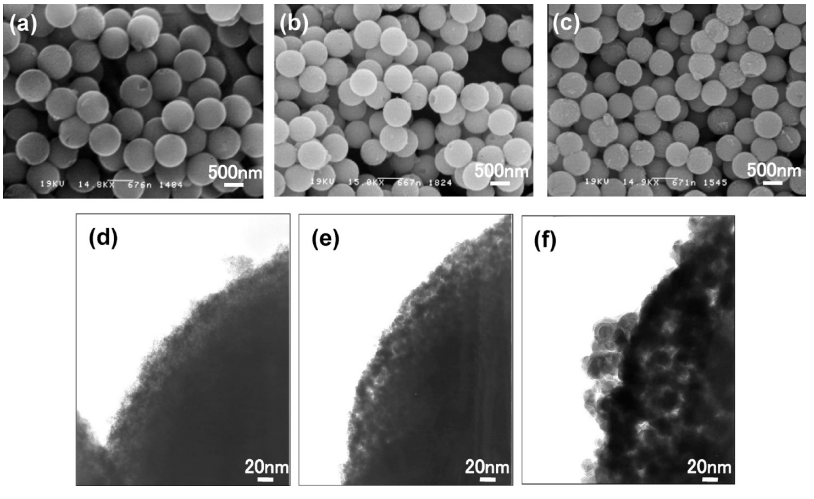

Figure 1. SEM images for (a) MSCS and MMTOS calcined at (b) 623 K and (c) 823 K and TEM images for (d) MSCS/SnO_2 composite, MMTOS calcined at (e) 623 K and (f) 823 K.

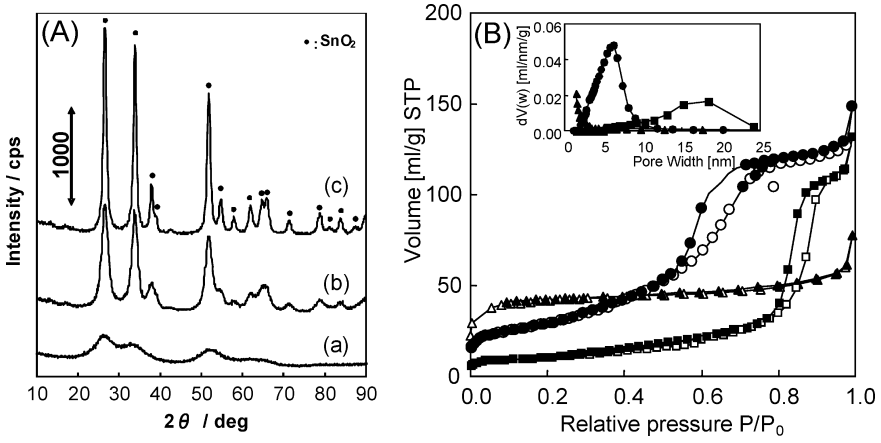

Figure 2. (A) XRD patterns for (a) MSCS/SnO_2 composite and MMTOS calcined at (b) 623 K and (c) 823 K. (B) Nitrogen adsorption−desorption isotherms for the MSCS/SnO_2 composite (filled and open triangles), MMTOS calcined at 623 K (filled and open circles), and MMTOS calcined at 823 K (filled and open squares). Inset in (B) shows pore size distribution curves for these materials evaluated by the BJH method from the adsorption branch.

MSCS through the oxidation of Sn^{2+} to Sn^{4+} in the acidic media, because Sn^{4+} is less soluble than Sn^{2+}. It is noteworthy that the precipitation of SnO_2 nanocrystals occurred only on MSCS. No isolated SnO_2 nanoparticles were found in the media. The crystalline size estimated by means of the Scherrer equation was about 2.0 nm. X-ray diffraction peaks for MMTOSs became bigger and sharper with the elevation of the calcination temperature. The crystalline sizes increased to 4.7 and 10.2 nm from 2.1 nm (the MSCS/SnO_2 composite) by calcination at 623 K and 823 K, respectively. These values agree well with those found in TEM images.

The nitrogen adsorption−desorption measurements were performed for the MSCS/SnO_2 composite and MMTOSs. Isotherms are shown in Figure 2B, and the total pore volume, the specific surface area, and the average pore diameter calculated from the isotherms are listed in Table 1. MSCS consists of carbon nanorods with a starburst structure, and nanospaces exist between the carbon nanorods.[27] The average size of the nanospaces was estimated to be 1.8 nm by the BJH method, well corresponding to the crystalline size of SnO_2 nanocrystals in the MSCS/SnO_2 composite calculated from the XRD pattern. The total pore volume of the MSCS/SnO_2 composite was 0.087 mL/g, which was almost 10% of that of MSCS, and no adsorption step due to pore filling is observed in the isotherm. From these results it is obvious that most mesopores of MSCS were filled with SnO_2 nanoparticles. Both of the isotherms for MMTOSs show steep increase arising from mesopore filling. The mesopores are considered to be generated upon the removal of carbon nanorods and subsequent aggregation of SnO_2 nanocrystals. By calcining the MSCS/SnO_2 composite at 623 K, MMTOS with 6.3 nm of pore diameter was obtained. The pore diameter expanded to 18 nm by raising the calcination temperature. It is found that the pore diameter can be tunable in some extent by changing the calcination temperature. The pore diameter of MMTOS increased with increasing calcination temperature, while the specific surface area decreased. As verified by TEM and XRD results, the crystalline sizes of

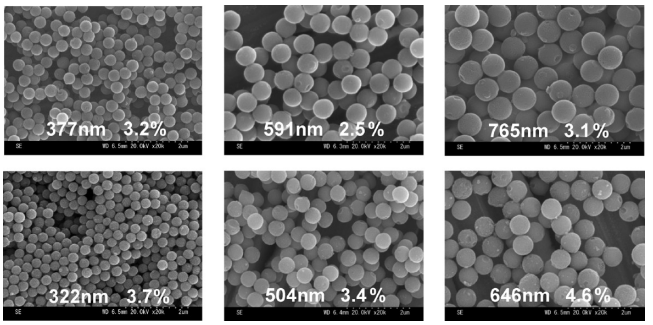

Figure 3. SEM images of MSCS with different particle diameters (upper images) and corresponding MMTOSs calcined at 623 K (lower images). An average particle diameter and CV are given in each image.

SnO_2 became larger when calcined at higher temperature, resulting in larger pore diameter and smaller specific surface area. MMTOSs had a relatively large specific surface area (35−103 m^2/g) and pore volume (0.17−0.19 mL/g), given the high mass density of SnO_2 (7.1 g/mL).

The advantage of our synthesis strategy is tunability in particle size. MMTOSs were synthesized by using MSCS with various diameters as templates to control the particle sizes of MMTOSs. Figure 3 shows SEM images of MSCS and resultant MMTOSs. It is clearly seen that MMTOSs with different particle diameters could be successfully obtained. Although the sizes of MMTOSs were approximately 20% smaller than that of MSCS, it is possible to obtain MMTOS with any size between 120 and 1200 nm, which is the size range obtained from MSCS with considering shrinkage. High resolution SEM observation for the smallest particles was conducted, and the image of a particle is shown in Figure 4. It is also confirmed that MMTOS with a particle size of 322 nm consists of SnO_2 nanoparticles. It is noteworthy that the particle size and mesopore diameter of MMTOS are tunable when our unique synthesis strategy is applied. It is very important to control the sizes of MMTOS for tuning the wavelength of a stop band of an opal fabricated from MMTOS for future photonic applications.

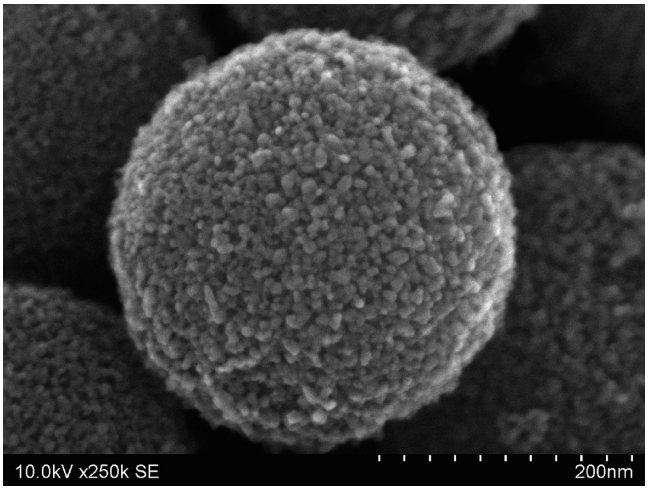

Figure 4. High resolution SEM image of MMTOS with the diameter of 322 nm. The image was obtained using a Hitachi S-5500N scanning electron microscope.

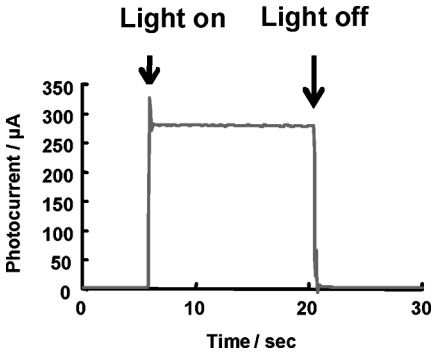

Figure 5. Photocurrent measured for Sn-TCPP incorporated MMTOS film. Photocurrent measurement was carried out by illuminating the sample with the light of a 420 nm wavelength.

Photocurrent Generation. Next, applicability of MMTOS for a dye sensitized solar cell was demonstrated by the incorporating porphyrin derivative, Sn-TCPP, into mesopores of MMTOS. Sn-TCPP has four carboxyl units which play an important role in stabilizing them inside mesopores by electrostatically binding the surface of MMTOS (Figure S1 in Supporting Information). Photocurrent measurement was performed using the photocurrent generation system illustrated in Figure S2 (Supporting Information). The result is presented in Figure 5. Illumination of the Sn-TCPP incorporated MMTOS with 420 nm wavelength light caused photocurrent, and the photocurrent turned to zero when the light was off. From Figure S2 (Supporting Information) it is considered that excited electrons of Sn-TCPP transferred to the conduction band of MMTOS and then photocurrent was generated. Incident photon to current conversion efficiency (IPCE) was calculated to be 0.15. This fact indicates that the aggregate of MMTOS was still conductive, although contact points between spheres or spheres and an FTO glass (substrate) were very restricted. It can be expected that IPCE would increase in large amount by optimizing particle size, pore diameter, crystallinity of MMTOS, types and the amount of a dye, and preparation method of a film. These issues are currently under investigation.

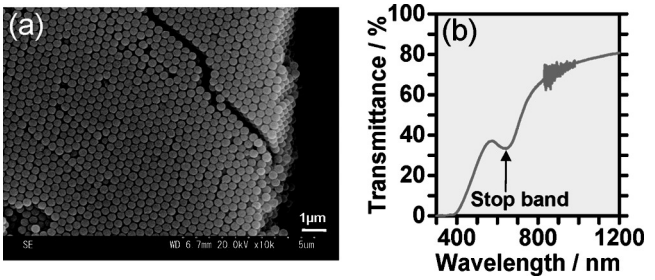

Figure 6. (a) SEM image of a colloidal photonic crystal obtained from MMTOS with the diameter of 322 nm. (b) Transmission spectrum of the colloidal photonic crystal showing a stop band around 650 nm.

Fabrication of Colloidal Photonic Crystal. One of the most important applications of monodispersed particles is to fabricate a colloidal photonic crystal for the production of novel photonic devices since unique properties such as light confinement effect and decrease in group velocity are expected in a photonic crystal due to the stop band effect. However, tin oxide has a high mass density (ca. 7 g/mL), and preparation of a stable dispersion is rather difficult, meaning that the fabrication of a colloidal photonic crystal with MMTOS is not so easy as being done with polystyrene or silica colloidal particles. Although we have several experiences in fabricating colloidal photonic crystals from monodispersed mesoporous silica spheres (MMSS) and their derivatives,[10−13,15] a colloidal photonic crystal could not be obtained from raw MMTOS. Then, MMTOS was coated with charged polymers and the fabrication of a colloidal photonic crystal was carried out. Figure 6 shows an SEM image of a colloidal photonic crystal obtained from the polymer coated MMTOS and its transmission spectrum. Particles of MMTOS contact each other and form a three-dimensionally close-packed opal structure. Although the surfaces of particles are coated with polymers, they are easily removed by combustion or extraction. The colloidal photonic crystal exhibits a stop band around 650 nm wavelength in its transmission spectrum as shown in Figure 6. The stop band wavelength of the colloidal photonic crystal can be tuned just by changing the particle size of MMTOS. This will be easily attained in our synthesis strategy by changing the particle size of the starting material, MMSS.

Conclusions

In summary, highly monodispersed mesoporous tin oxide spheres (MMTOS) have been successfully obtained using monodispersed starburst carbon spheres (MSCS) as a host. Particle size and mesopore diameter of MMTOS can easily be tuned by changing the size of parent MSCS and the calcination temperature. Photocurrent generation was demonstrated for Sn-TCPP incorporated MMTOS by illuminating light of 420 nm wavelength. In addition, it was found that a colloidal photonic crystal exhibiting a stop band could be obtained from

mesoporous tin oxide spheres for the first time. Our new strategy can be applied to other semiconductor materials, such as titania, indicating that other types of conductive monodispersed mesoporous spheres and their opals can be obtained. It is quite possible to incorporate a variety of dyes, polymers, and nanoparticles into mesopores of MMTOS. We believe that the combination of MMTOS and materials incorporated enables us to create novel photonic devices, such as optically amplified solar cells or zero-threshold lasers, by taking advantage of both the unique property of a photonic crystal and conductive characteristics. Work is underway to investigate the effect of a stop band on photocurrent in a dye sensitized solar cell system.

Supporting Information Available: (1) Chemical structure, diffuse reflectance spectrum, and fluorescence spectrum of Sn-TCPP. (2) Schematic illustration of photocurrent generation system for Sn-TCPP/MMTOS (PDF). This material is available free of charge via the Internet at http://pubs.acs.org.